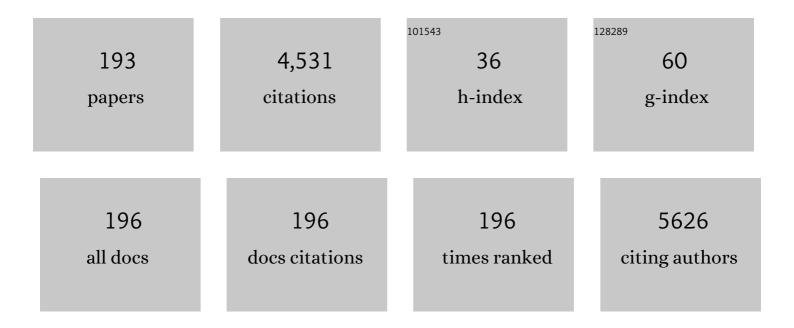
## List of Publications by Year in descending order

Source: https://exaly.com/author-pdf/7802483/publications.pdf Version: 2024-02-01



ALAY SINCH

#	Article	IF	CITATIONS
1	Conductive polymers for thermoelectric power generation. Progress in Materials Science, 2018, 93, 270-310.	32.8	274
2	Key issues in development of thermoelectric power generators: High figure-of-merit materials and their highly conducting interfaces with metallic interconnects. Energy Conversion and Management, 2016, 114, 50-67.	9.2	231
3	Realization of High Thermoelectric FigureÂof Merit in GeTe by Complementary Co-doping of Bi and In. Joule, 2019, 3, 2565-2580.	24.0	175
4	Improved thermoelectric performance of hot pressed nanostructured n-type SiGe bulk alloys. Journal of Materials Chemistry A, 2014, 2, 6922.	10.3	145
5	Nanostructured Boron Nitride With High Water Dispersibility For Boron Neutron Capture Therapy. Scientific Reports, 2016, 6, 35535.	3.3	124
6	XPS and AFM investigations of annealing induced surface modifications of MgO single crystals. Journal of Crystal Growth, 2002, 236, 661-666.	1.5	120
7	Nano-crystalline Fe2O3 thin films for ppm level detection of H2S. Sensors and Actuators B: Chemical, 2013, 181, 471-478.	7.8	110
8	H2S sensing using in situ photo-polymerized polyaniline–silver nanocomposite films on flexible substrates. Organic Electronics, 2014, 15, 71-81.	2.6	102
9	CuCrSe2: a high performance phonon glass and electron crystal thermoelectric material. Journal of Materials Chemistry A, 2013, 1, 11289.	10.3	85
10	High thermoelectric performance of (AgCrSe <sub>2</sub> ) <sub>0.5</sub> (CuCrSe <sub>2</sub> ) <sub>0.5</sub> nano-composites having all-scale natural hierarchical architectures. Journal of Materials Chemistry A, 2014, 2, 17122-17129.	10.3	82
11	Boosting thermoelectric performance of p-type SiGe alloys through in-situ metallic YSi2 nanoinclusions. Nano Energy, 2016, 27, 282-297.	16.0	79
12	Flexible H2S sensor based on gold modified polycarbazole films. Sensors and Actuators B: Chemical, 2014, 200, 227-234.	7.8	78
13	Enhanced H2S sensing characteristics of Au modified Fe2O3 thin films. Sensors and Actuators B: Chemical, 2015, 219, 125-132.	7.8	77
14	Photo-induced synthesis of polypyrrole-silver nanocomposite films on N-(3-trimethoxysilylpropyl)pyrrole-modified biaxially oriented polyethylene terephthalate flexible substrates. RSC Advances, 2013, 3, 5506.	3.6	76
15	Chemiresistive gas sensing properties of nanocrystalline Co3O4 thin films. Sensors and Actuators B: Chemical, 2013, 176, 38-45.	7.8	74
16	Development of low resistance electrical contacts for thermoelectric devices based on n-type PbTe and p-type TAGS-85 ((AgSbTe <sub>2</sub> ) <sub>0.15</sub> (GeTe) <sub>0.85</sub> ). Journal Physics D: Applied Physics, 2009, 42, 015502.	2.8	73
17	NO2 sensors with room temperature operation and long term stability using copper phthalocyanine thin films. Sensors and Actuators B: Chemical, 2009, 143, 246-252.	7.8	72
18	An alternative method of preparation of dosimetric grade α-Al2O3:C by vacuum-assisted post-growth thermal impurification technique. Radiation Measurements, 2005, 39, 277-282.	1.4	63

#	Article	IF	CITATIONS
19	Mode-Selective Excited-State Proton Transfer in 2-(2â€~-Pyridyl)pyrrole Isolated in a Supersonic Jet. Journal of the American Chemical Society, 2007, 129, 2738-2739.	13.7	61
20	Room temperature detection of H2S by flexible gold–cobalt phthalocyanine heterojunction thin films. Sensors and Actuators B: Chemical, 2015, 206, 653-662.	7.8	59
21	Fast Response and High Sensitivity of ZnO Nanowires—Cobalt Phthalocyanine Heterojunction Based H2S Sensor. ACS Applied Materials & Interfaces, 2015, 7, 17713-17724.	8.0	57
22	One step synthesis of highly ordered free standing flexible polypyrrole-silver nanocomposite films at air–water interface by photopolymerization. RSC Advances, 2013, 3, 13329.	3.6	56
23	Electrochemical investigation of free-standing polypyrrole–silver nanocomposite films: a substrate free electrode material for supercapacitors. RSC Advances, 2013, 3, 24567.	3.6	55
24	Proton transfer with a twist? Femtosecond Dynamics of 7â€(2â€pyridyl)indole in Condensed Phase and in Supersonic Jets. Angewandte Chemie - International Edition, 2008, 47, 6037-6040.	13.8	54
25	Degradation behavior of MgB2 superconductor. Physica C: Superconductivity and Its Applications, 2001, 363, 208-214.	1.2	53
26	Temperature dependent H2S and Cl2 sensing selectivity of Cr2O3 thin films. Sensors and Actuators B: Chemical, 2011, 157, 466-472.	7.8	53
27	Flexible organic semiconductor thin films. Journal of Materials Chemistry C, 2015, 3, 8468-8479.	5.5	51
28	Superconducting spin switch with perpendicular magnetic anisotropy. Physical Review B, 2007, 75, .	3.2	49
29	One-step UV-induced modification of cellulose fabrics by polypyrrole/silver nanocomposite films. Journal of Colloid and Interface Science, 2013, 393, 130-137.	9.4	49
30	Core/shell, protuberance-free multiwalled carbon nanotube/polyaniline nanocomposites via interfacial chemistry of aryl diazonium salts. Journal of Colloid and Interface Science, 2014, 418, 185-192.	9.4	47
31	Surface and interface physicochemical aspects of intercalated organo-bentonite. International Journal of Adhesion and Adhesives, 2014, 50, 204-210.	2.9	43
32	Flexo-green Polypyrrole – Silver nanocomposite films for thermoelectric power generation. Energy Conversion and Management, 2017, 144, 143-152.	9.2	41
33	Synergetic effect of CuS@ZnS nanostructures on photocatalytic degradation of organic pollutant under visible light irradiation. RSC Advances, 2017, 7, 34366-34375.	3.6	40
34	Growth of iron phthalocyanine nanoweb and nanobrush using molecular beam epitaxy. Physica E: Low-Dimensional Systems and Nanostructures, 2008, 41, 154-163.	2.7	39
35	Transition from n- to p-type conduction concomitant with enhancement of figure-of-merit in Pb doped bismuth telluride: Material to device development. Materials and Design, 2018, 159, 127-137.	7.0	39
36	Bending stress induced improved chemiresistive gas sensing characteristics of flexible cobalt-phthalocyanine thin films. Applied Physics Letters, 2013, 102, .	3.3	38

#	Article	IF	CITATIONS
37	Free-standing flexible multiwalled carbon nanotubes paper for wearable thermoelectric power generator. Journal of Power Sources, 2020, 449, 227493.	7.8	38
38	High temperature Si–Ge alloy towards thermoelectric applications: A comprehensive review. Materials Today Physics, 2021, 21, 100468.	6.0	38
39	Tellurium-free thermoelectrics: Improved thermoelectric performance of n-type Bi 2 Se 3 having multiscale hierarchical architecture. Energy Conversion and Management, 2017, 145, 415-424.	9.2	37
40	Novel, ternary clay/polypyrrole/silver hybrid materials through in situ photopolymerization. Colloids and Surfaces A: Physicochemical and Engineering Aspects, 2013, 439, 193-199.	4.7	36
41	Improved performance of dye sensitized solar cell via fine tuning of ultra-thin compact TiO 2 layer. Solar Energy Materials and Solar Cells, 2017, 170, 127-136.	6.2	36
42	Spin-polarized current versus stray field in a perpendicularly magnetized superconducting spin switch. Applied Physics Letters, 2007, 91, 152504.	3.3	35
43	Parts-per-billion level chlorine sensors with fast kinetics using ultrathin cobalt phthalocyanine films. Chemical Physics Letters, 2009, 480, 185-188.	2.6	35
44	Growth of Pd4S, PdS and PdS2 films by controlled sulfurization of sputtered Pd on native oxide of Si. Thin Solid Films, 2013, 539, 41-46.	1.8	35
45	Nanostructured polypyrrole: enhancement in thermoelectric figure of merit through suppression of thermal conductivity. Materials Research Express, 2017, 4, 085007.	1.6	34
46	Anisotropic electrical transport studies of Ca3Co4O9 single crystals grown by the flux method. Journal of Crystal Growth, 2005, 277, 246-251.	1.5	33
47	Effect of grain boundaries on paraconductivity of YBa 2 Cu 3 O x. Journal of Physics and Chemistry of Solids, 2002, 63, 1797-1803.	4.0	32
48	Room temperature ppb level Cl2 sensing using sulphonated copper phthalocyanine films. Talanta, 2010, 82, 1485-1489.	5.5	31
49	Exfoliated clay/polyaniline nanocomposites through tandem diazonium cation exchange reactions and in situ oxidative polymerization of aniline. RSC Advances, 2014, 4, 65213-65222.	3.6	30
50	Ultrasensitive and Selective Detection of Dopamine Using Cobalt-Phthalocyanine Nanopillar-Based Surface Acoustic Wave Sensor. ACS Applied Materials & Interfaces, 2014, 6, 22378-22386.	8.0	30
51	Bias and temperature dependent charge transport in high mobility cobalt-phthalocyanine thin films. Applied Physics Letters, 2010, 96, .	3.3	29
52	In Situ Diazonium-Modified Flexible ITO-Coated PEN Substrates for the Deposition of Adherent Silver–Polypyrrole Nanocomposite Films. Langmuir, 2014, 30, 9397-9406.	3.5	28
53	Scalable free-standing polypyrrole films for wrist-band type flexible thermoelectric power generator. Energy, 2019, 176, 853-860.	8.8	27
54	Room temperature ammonia sensor based on jaw like bis-porphyrin molecules. Organic Electronics, 2013, 14, 1189-1196.	2.6	26

#	Article	IF	CITATIONS
55	7-Pyridylindoles:Â Synthesis, Structure, and Properties. Journal of Organic Chemistry, 2006, 71, 7611-7617.	3.2	25
56	Low temperature thermoelectric properties of Cu intercalated TiSe2: a charge density wave material. Applied Physics A: Materials Science and Processing, 2013, 111, 465-470.	2.3	24
57	Synthesis and characterization of MgB2 superconductor. Physica C: Superconductivity and Its Applications, 2001, 363, 149-154.	1.2	23
58	Electron beam induced modifications of polyaniline silver nano-composite films: Electrical conductivity and H2S gas sensing studies. Radiation Physics and Chemistry, 2018, 153, 131-139.	2.8	23
59	Structure and Photophysics of 2-(2â€~-Pyridyl)benzindoles:  The Role of Intermolecular Hydrogen Bonds. Journal of Physical Chemistry A, 2007, 111, 11400-11409. Electronic transport in magnetically ordered <mml:math< td=""><td>2.5</td><td>22</td></mml:math<>	2.5	22
60	xmlns:mml="http://www.w3.org/1998/Math/MathML" display="inline"> <mml:mrow><mml:msub><mml:mi mathvariant="normal"&gt;Mn<mml:mn>5</mml:mn></mml:mi </mml:msub><mml:msub><mml:mi mathvariant="normal"&gt;Si<mml:mn>3</mml:mn></mml:mi </mml:msub><mml:msub><mml:mi mathvariant="normal"&gt;C<mml:mi>x</mml:mi></mml:mi </mml:msub></mml:mrow> films.	3.2	22
61	Physical Review B, 2008, 77, Enhanced Cl <sub>2</sub> sensitivity of cobalt-phthalocyanine film by utilizing a porous nanostructured surface fabricated on glass. RSC Advances, 2017, 7, 4135-4143.	3.6	22
62	High energy electron beam induced improved thermoelectric properties of PEDOT:PSS films. Polymer, 2020, 202, 122645.	3.8	22
63	Oxygen induced hysteretic current-voltage characteristics of iron-phthalocyanine thin films. Journal of Applied Physics, 2008, 104, .	2.5	21
64	Enhanced Thermoelectric Properties of Selenium-Deficient Layered TiSe <sub>2–<i>x</i></sub> : A Charge-Density-Wave Material. ACS Applied Materials & Interfaces, 2014, 6, 18619-18625.	8.0	21
65	Boosting thermoelectric power factor of free-standing Poly(3,4ethylenedioxythiophene):polystyrenesulphonate films by incorporation of bismuth antimony telluride nanostructures. Journal of Power Sources, 2019, 435, 226758.	7.8	21
66	Broadband enhancement in absorption cross-section of N719 dye using different anisotropic shaped single crystalline silver nanoparticles. RSC Advances, 2016, 6, 48064-48071.	3.6	20
67	Bis-porphyrin films as ppb level chemiresistive sensors. Chemical Physics Letters, 2010, 488, 27-31.	2.6	19
68	Low temperature processable ultra-thin WO3 Langmuir-Blodgett film as excellent hole blocking layer for enhanced performance in dye sensitized solar cell. Electrochimica Acta, 2019, 318, 405-412.	5.2	19
69	Magnetic field dependent microwave absorption studies on a MgB2superconductor. Superconductor Science and Technology, 2001, 14, 572-575.	3.5	18
70	Role of structural disorder in charge transport properties of cobalt phthalocyanine thin films grown by molecular-beam epitaxy. Organic Electronics, 2010, 11, 1835-1843.	2.6	18
71	Thermoelectric performance of Cu intercalated layered TiSe2 above 300 K. Journal of Applied Physics, 2013, 114, .	2.5	17
72	Study of thermal stability of Cu2Se thermoelectric material. AIP Conference Proceedings, 2016, , .	0.4	17

#	Article	IF	CITATIONS
73	Enhanced thermoelectric figure-of-merit of p-type SiGe through TiO2 nanoinclusions and modulation doping of boron. Materialia, 2018, 4, 147-156.	2.7	17
74	Charge transport in polypyrrole:ZnO-nanowires composite films. Applied Physics Letters, 2009, 95, 202106.	3.3	16
75	Implication of molecular orientation on charge transport and gas sensing characteristics of cobalt–phthalocyanine thin films. Organic Electronics, 2012, 13, 2600-2604.	2.6	16
76	Defect profiling in organic semiconductor multilayers. Organic Electronics, 2012, 13, 1409-1419.	2.6	16
77	Electron density profile at the interfaces of bulk heterojunction solar cells and its implication on the S-kink characteristics. Chemical Physics Letters, 2016, 646, 6-11.	2.6	15
78	Anisotropy of critical current density inc-axis-orientedMgB2thin films. Physical Review B, 2002, 65, .	3.2	14
79	Ferromagnetic resonance studies of nanocrystalline La0.6Pb0.4MnO3 thin films. Materials Letters, 2005, 59, 728-733.	2.6	14
80	Melt processing of alumina in graphite ambient for dosimetric applications. Journal of Luminescence, 2008, 128, 445-450.	3.1	14
81	Improved Thermoelectric Properties of Se-Doped n-Type PbTe1â^'x Se x (0Ââ‰ÂxÂâ‰Â1). Journal of Electronic Materials, 2013, 42, 2292-2296.	2.2	14
82	Charge transport and ammonia sensing properties of flexible polypyrrole nanosheets grown at air–liquid interface. Materials Chemistry and Physics, 2013, 140, 300-306.	4.0	14
83	Electron Beam Modified Organic Materials and their Applications. Solid State Phenomena, 0, 239, 72-97.	0.3	14
84	Elucidating the mechanisms behind thermoelectric power factor enhancement of poly(3,4-ethylenedioxythiophene):poly(styrenesulfonate) flexible films. Vacuum, 2018, 153, 238-247.	3.5	14
85	Remarkable Improvement of Thermoelectric Figure-of-Merit in SnTe through In Situ-Created Te Nanoinclusions. ACS Applied Energy Materials, 2020, 3, 7113-7120.	5.1	14
86	lâ^'Vcharacteristic measurements to study the nature of the vortex state and dissipation inMgB2thin films. Physical Review B, 2002, 66, .	3.2	13
87	Modeling of gate bias controlled NO2 response of the PCDTBT based organic field effect transistor. Chemical Physics Letters, 2018, 698, 7-10.	2.6	13
88	Synergistic effect of Zn doping on thermoelectric properties to realize a high figure-of-merit and conversion efficiency in Bi <sub>2â~<i>x</i></sub> Zn <sub><i>x</i></sub> Te <sub>3</sub> based thermoelectric generators. Journal of Materials Chemistry C, 2022, 10, 7970-7979.	5.5	13
89	Metallic-like conduction in Co-phthalocyanine/Fe-phthalocyanine composite films grown on sapphire substrates. Applied Physics Letters, 2011, 99, .	3.3	12
90	Electron beam induced modifications in flexible biaxially oriented polyethylene terephthalate sheets: Improved mechanical and electrical properties. Materials Chemistry and Physics, 2017, 189, 237-244.	4.0	12

#	Article	IF	CITATIONS
91	Electron beam modified zinc phthalocyanine thin films for radiation dosimeter application. Synthetic Metals, 2017, 231, 143-152.	3.9	12
92	Stabilizing Thermoelectric Figureâ€ofâ€Merit of Superionic Conductor Cu <sub>2</sub> Se through W Nanoinclusions. Physica Status Solidi - Rapid Research Letters, 2020, 14, 2000102.	2.4	12
93	Low temperature thermopower and electrical transport in misfit Ca3Co4O9with elongatedc-axis. Journal Physics D: Applied Physics, 2008, 41, 085414.	2.8	11
94	Flexible cobalt-phthalocyanine thin films with high charge carrier mobility. Applied Physics Letters, 2012, 101, .	3.3	11
95	Anionic conduction mediated giant n-type Seebeck coefficient in doped Poly(3-hexylthiophene) free-standing films. Materials Today Physics, 2021, 16, 100307.	6.0	11
96	Positron annihilation studies in theMgB2superconductor. Physical Review B, 2002, 66, .	3.2	10
97	Enhanced magnetoresistance in nanocrystalline La0.6Pb0.4MnO3 thin films. Journal of Crystal Growth, 2002, 244, 313-317.	1.5	10
98	Growth and morphology of the single crystals of thermoelectric oxide material NaxCoO2. Crystal Research and Technology, 2004, 39, 572-576.	1.3	10
99	Tunneling characteristics and resistivity behavior ofLa0.6Pb0.4MnO3grain boundaries. Physical Review B, 2006, 73, .	3.2	10
100	16S rRNA and Omp31 Gene Based Molecular Characterization of Field Strains ofB. melitensisfrom Aborted Foetus of Goats in India. Scientific World Journal, The, 2013, 2013, 1-7.	2.1	10
101	Growth of epitaxial multilayers consisting of alternately stacked superconducting YBa2Cu3O7â^î^and colossal magnetoresistive La1â^'xPbxMnO3 layers. Journal of Crystal Growth, 2002, 243, 134-142.	1.5	9
102	Ground and excited state vibrations of 2-(2′-pyridyl)pyrrole. Journal of Molecular Structure, 2007, 844-845, 286-299.	3.6	9
103	Improved charge conduction in cobalt-phthalocyanine thin films grown along 36.8Ű boundary of SrTiO3 bicrystals. Applied Physics Letters, 2011, 98, .	3.3	9
104	Synthesis and characterization of sol-gel derived Cr2O3 nanoparticles. AIP Conference Proceedings, 2012, , .	0.4	9
105	Fluorinated copper-phthalocyanine/cobalt-phthalocyaine organic heterojunctions: Charge transport and Kelvin probe studies. Applied Physics Letters, 2012, 100, .	3.3	9
106	Enhanced Cl2 response of ultrathin bi-nuclear (cobalt–iron) phthalocyanine films. Sensors and Actuators B: Chemical, 2012, 171-172, 423-430.	7.8	8
107	Structural and Magnetic Depth Profiling and Their Correlation in Self-Assembled Co and Fe Based Phthalocyanine Thin Films. Journal of Physical Chemistry C, 2014, 118, 4072-4077.	3.1	8
108	Polyanilineâ€Wrapped ZnO Nanorod Composite Films on Diazoniumâ€Modified Flexible Plastic Substrates. Macromolecular Chemistry and Physics, 2016, 217, 1136-1148.	2.2	8

#	Article	IF	CITATIONS
109	Design and development of DC to DC voltage booster to integrate with PbTe/TAGS-85 based thermoelectric power generators. Materials Science for Energy Technologies, 2019, 2, 429-433.	1.8	8
110	A synergistic approach to achieving the high thermoelectric performance of La-doped SnTe using resonance state and partial band convergence. Materials Advances, 2021, 2, 4352-4361.	5.4	8
111	Magneto-transport and ferromagnetic resonance studies of polycrystalline La0.6Pb0.4MnO3 thin films. Solid State Communications, 2006, 137, 456-461.	1.9	7
112	Band Convergence and Phonon Scattering Mediated Improved Thermoelectric Performance of SnTe–PbTe Nanocomposites. ACS Applied Energy Materials, 2020, 3, 8882-8891.	5.1	7
113	Polypyrrole/Ag Nanocomposite Films on Diazonium Salt Modified Indium Tin Oxide Substrate. Journal of Colloid Science and Biotechnology, 2013, 2, 200-210.	0.2	7
114	Manipulating superconductivity in perpendicularly magnetized FSF triple layers. Applied Physics A: Materials Science and Processing, 2007, 89, 593-597.	2.3	6
115	Micro-structural characterization of low resistive metallic Ni germanide growth on annealing of Ni-Ge multilayer. AIP Advances, 2015, 5, .	1.3	6
116	Optimization of Thermoelectric Properties of Mechanically Alloyed p-Type SiGe by Mathematical Modelling. Journal of Electronic Materials, 2019, 48, 649-655.	2.2	6
117	Self-Operating Flyback Converter for Boosting Ultra-Low Voltage of Thermoelectric Power Generator for IoT Applications. IEEE Transactions on Industrial Electronics, 2022, 69, 12957-12966.	7.9	6
118	Andreev reflections on aMgB2superconductor. Physical Review B, 2002, 66, .	3.2	5
119	In-plane and out-of-plane anisotropic magnetoresistances in La1 â^'xPbxMnO3thin films. Philosophical Magazine, 2003, 83, 3181-3191.	1.6	5
120	Magnetization and magnetotransport studies of Y Ba2Cu3O7ÂÂ/La1ÂxPbxMnO3heterostructures. Superconductor Science and Technology, 2004, 17, 342-346.	3.5	5
121	Magneto-transport properties of nano-crystalline and poly-crystalline La0.6Pb0.4MnO3 thin films. Journal of Magnetism and Magnetic Materials, 2007, 313, 115-121.	2.3	5
122	Effect of Te doping on the thermopower of PbSe <sub>1–x</sub> Te <sub>x</sub> . Emerging Materials Research, 2012, 1, 306-311.	0.7	5
123	Thermoelectric properties of AgCrSe2. AIP Conference Proceedings, 2012, , .	0.4	5
124	Thermoelectric performance of layered Sr <sub>x</sub> TiSe <sub>2</sub> above 300 K. Journal of Physics Condensed Matter, 2014, 26, 445002.	1.8	5
125	Electron beam induced modifications in electrical properties of Poly(3,4-ethylenedioxythiophene):poly(styrenesulfonate) films. Vacuum, 2018, 152, 243-247.	3.5	5
126	Radiation-resistant beta-photovoltaic battery using Ce-doped Gd3Ga3Al2O12 single-crystal scintillator. Applied Physics Letters, 2021, 118, .	3.3	5

#	Article	IF	CITATIONS
127	Electromagnetic interference shielding effectiveness of polypyrrole-silver nanocomposite films on silane-modified flexible sheet. High Performance Polymers, 2022, 34, 310-320.	1.8	5
128	Low current induced electroresistance in the polycrystalline La0.6Pb0.4MnO3 thin films. Journal of Applied Physics, 2007, 102, 043907.	2.5	4
129	Surface acoustic wave sensor based on nickel(II) phthalocyanine thin films for organophosphorous pesticides selective detection. , 2014, , .		4
130	Effect of ball milling time on thermoelectric properties of bismuth telluride nanomaterials. AIP Conference Proceedings, 2018, , .	0.4	4
131	Synergistic manifestation of band and scattering engineering in single aliovalent Sb alloyed anharmonic SnTe alloy in concurrence with rule of parsimony. Materials Advances, 0, , .	5.4	4
132	Comparative H <sub>2</sub> S Sensing Characteristics of Fe <sub>2</sub> 0 <sub>3</sub> : Thin Film vs. Bulk. Soft Nanoscience Letters, 2013, 03, 6-8.	0.8	4
133	Correlation between extrinsic magnetoresistance and electroresistance in La0.6Pb0.4MnO3 thin films as revealed from current–voltage and ferromagnetic resonance studies. Solid State Communications, 2006, 138, 430-435.	1.9	3
134	Study of iron phthalocyanine organic semiconductor thin films using slow positron beam. Physica Status Solidi C: Current Topics in Solid State Physics, 2009, 6, 2589-2591.	0.8	3
135	Influence of adsorbed oxygen on charge transport and chlorine gas-sensing characteristics of thin cobalt phthalocyanine films. Chemical Papers, 2012, 66, .	2.2	3
136	Thermoelectric properties of Ag added Ca0.98La0.02MnO3. , 2014, , .		3
137	Morphologyâ€Ðriven Sensitivity Enhancement of MEHâ€PPV Langmuirâ€Blodgett Films on Plastic Substrates for NO <sub>2</sub> Gas. ChemistrySelect, 2018, 3, 188-194.	1.5	3
138	Temperature Driven Unusual Reversible p―to nâ€Type Conduction Switching in Bi 2 Te 2.7 Se 0.3. Physica Status Solidi - Rapid Research Letters, 2019, 13, 1900121.	2.4	3
139	Electron Beam Induced Tailoring of Electrical Characteristics of Organic Semiconductor Films. Chemistry Africa, 2020, 3, 571-592.	2.4	3
140	Bismuth Telluride Based Efficient Thermoelectric Power Generator with Electrically Conducive Interfaces for Harvesting Low Temperature Heat. Journal of Science: Advanced Materials and Devices, 2022, , 100447.	3.1	3
141	Phase Variation of Ultrathin WO <sub>3</sub> Electronâ€Transport Layer Prepared by Scalable Langmuir–Blodgett Technique to Boost Efficiency of Dye Sensitized Solar Cells. Solar Rrl, 2022, 6, .	5.8	3
142	Temperature Dependent Current–Voltage Characteristics of Iron-Phthalocyanine Thin Films. Journal of Nanoscience and Nanotechnology, 2009, 9, 5262-5267.	0.9	2
143	Spintronics in metallic superconductor/ferromagnet hybrid structures. International Journal of Materials Research, 2010, 101, 164-174.	0.3	2
144	Effect of hot-press sintering temperature on thermal transport properties of TiSe[sub 2]. , 2013, , .		2

#	Article	IF	CITATIONS
145	Thermoelectric properties of CuCrSe[sub 2]. , 2013, , .		2
146	Growth and Electrical Transport Properties of Organic Semiconductor Thin Films. Solid State Phenomena, 2013, 209, 1-5.	0.3	2
147	Trap Free Space Charge Limited Conduction and High Mobility in Cobalt Phthalocyanine - Iron Phthalocyanine Composite Thin Films. Solid State Phenomena, 2013, 209, 52-56.	0.3	2
148	Enhanced H[sub 2]S response of Au modified Fe[sub 2]O[sub 3] thin films. , 2013, , .		2
149	Improvement in thermoelectric power factor of mechanically alloyed p-type SiGe by incorporation of TiB2. AIP Conference Proceedings, 2016, , .	0.4	2
150	Improving the Thermoelectric Performance of Tetrahedrally Bonded Quaternary Selenide Cu2CdSnSe4 Using CdSe Precipitates. Journal of Electronic Materials, 2019, 48, 2120-2130.	2.2	2
151	Tailoring of thermoelectric properties in Bi2Te3 by varying the sintering temperature. AIP Conference Proceedings, 2020, , .	0.4	2
152	Flexible, Biocompatible PET Sheets: A Platform for Attachment, Proliferation and Differentiation of Eukaryotic Cells. Surfaces, 2021, 4, 306-322.	2.3	2
153	Preparation and characterization of MgB2 superconductor. Pramana - Journal of Physics, 2002, 58, 867-870.	1.8	1
154	Effect of substrate temperature on electrical and magnetic properties of epitaxial La1â^'x Pb x MnO3 films. Pramana - Journal of Physics, 2002, 58, 1065-1067.	1.8	1
155	Colossal magnetoresistance in layered manganite Nd2â^'2x Sr1+2x Mn2O7 (0 ≤ ≤0.5). Pramana - Journal of Physics, 2002, 58, 1085-1088.	1.8	1
156	Molecular Beam Epitaxy Growth of Iron Phthalocyanine Nanostructures. , 2009, , .		1
157	Charge transport in ultrathin iron-phthalocyanine thin films under high electric fields. Journal of Physics Condensed Matter, 2011, 23, 355801.	1.8	1
158	Thermoelectric Properties of Ca[sub 4]Mn[sub 3â^`x]Nb[sub x]O[sub 10]. , 2011, , .		1
159	Metal–semiconductor transition in ultrathin cobalt-phthalocyanine films grown on SrTiO3single crystal substrates. Applied Physics Letters, 2012, 100, 162101.	3.3	1
160	Thermoelectric properties of transition metal intercalated layered TiSe2. , 2012, , .		1
161	Influence of Cu intercalation on thermal transport properties of titanium diselenide. , 2013, , .		1
162	Thermal transport properties of strontium intercalated titanium diselenide. , 2013, , .		1

10

#	Article	IF	CITATIONS
163	Enhanced figure of merit in (AgCrSe[sub 2])[sub 0.75](CuCrSe[sub 2])[sub 0.25]. AIP Conference Proceedings, 2013, , .	0.4	1
164	Cobalt phthalocyanine/ZnO nanowire heterojunction film for H2S sensor. AIP Conference Proceedings, 2015, , .	0.4	1
165	Optimisation of electrical contact resistance in Bi0.5Sb1.5Te3 for development of thermoelectric generators. AIP Conference Proceedings, 2017, , .	0.4	1
166	Tailoring thermal conductivity in PbS by incorporation of copper for thermoelectric applications. AIP Conference Proceedings, 2017, , .	0.4	1
167	Lead sulphide: Low cost, abundant thermoelectrics. AIP Conference Proceedings, 2018, , .	0.4	1
168	Effect of tin on thermoelectric power factor of indium tin oxide. AIP Conference Proceedings, 2019, , .	0.4	1
169	Near room temperature thermoelectrics: Ag2Se. AIP Conference Proceedings, 2020, , .	0.4	1
170	Microwave absorption studies of MgB2 superconductor. Pramana - Journal of Physics, 2002, 58, 799-802.	1.8	0
171	Electrical And Positron Study Of The Interface Of Organic Semiconductor Heterojunction. , 2010, , .		0
172	Charge Transport Characteristics Of Cobalt Phthalocyanine Thin Films Grown By Molecular Beam Epitaxy. , 2010, , .		0
173	Study of interfaces in organic semiconductor heterojunctions. Journal of Physics: Conference Series, 2011, 262, 012036.	0.4	Ο
174	Mechanism of Charge Transport in Cobalt and Iron Phthalocyanine Thin Films Grown by Molecular Beam Epitaxy. , 2011, , .		0
175	Ordering Induced Enhancement of Charge Carrier Mobility In CoPc Thin Films. , 2011, , .		0
176	Implication of Structural Disorder in The Charge Transport Properties of Cobalt-phthalocyanine Thin Films. , 2011, , .		0
177	Reverse rectification behavior of NiPc (p-type)/F16CuPc (n-type) heterojunction. , 2012, , .		Ο
178	Improved thermoelectric properties of PbTe0.5Se0.5. , 2012, , .		0
179	Chemi-resistive gas sensing properties of cobalt-phthalocyanine / iron-phthalocyanine composite films. , 2012, , .		0
180	Dramatic thermal conductivity reduction in PbSe[sub 0.5]Te[sub 0.5]. , 2013, , .		0

#	Article	IF	CITATIONS
181	Electron accumulation/depletion at F[sub 16]CoPc/Znq[sub 3] heterojunction: Kelvin probe and charge transport study. , 2013, , .		0
182	Iodine doped polyaniline and cobalt-phthalocyanine as sensitive layers for ammonia detection via surface acoustic wave sensor. , 2014, , .		0
183	High temperature thermoelectric performance of NiCr2Se4. AIP Conference Proceedings, 2015, , .	0.4	0
184	Interface mediated semiconducting to metallic like transition in ultrathin Bi2Se3 films on (100) SrTiO3 grown by molecular beam epitaxy. RSC Advances, 2015, 5, 87897-87902.	3.6	0
185	Studies on different configurations of cobalt phthalocyanine based flexible organic field effect transistor. AIP Conference Proceedings, 2016, , .	0.4	0
186	Chemical synthesis and characterization of PdTe-Ag2Te nanowires heterostructure. AIP Conference Proceedings, 2016, , .	0.4	0
187	Synthesis & tailoring the thermal conductivity of Sr doped Bi2Se3 thermoelectric material. AIP Conference Proceedings, 2017, , .	0.4	0
188	Carbon doping-induced defect centers in anodized alumina with enhanced optically stimulated luminescence. Journal of Materials Science: Materials in Electronics, 2021, 32, 10635-10643.	2.2	0
189	ELECTROGRAFTING OF ORGANIC MONOLAYERS ON SILICON FOR MOLECULAR ELECTRONICS. , 2007, , .		0
190	Ambient-air fabrication with inorganic/polymer hole transport layer: Towards low cost perovskite solar cells. AIP Conference Proceedings, 2020, , .	0.4	0
191	Environment friendly SnTe thermoelectrics: Material to device. AIP Conference Proceedings, 2020, , .	0.4	0
192	Low temperature processable crystalline WO3 Langmuir-Blodgett ultra-thin film as blocking layer in solar cells application. AIP Conference Proceedings, 2020, , .	0.4	0
193	Thermoelectric power generation from the perspective of conducting polymers. AIP Conference Proceedings, 2020, , .	0.4	0